Confidential document: To be submitted to New Phytologist

Marine macroalgae are an overlooked sink of Si in coastal systems

Mollie Yacano[1,2], Sarah Q. Foster[1,8], Nicholas E. Ray[3], Autumn Oczkowski[4], John A. Raven[5-7], Robinson W. Fulweiler[1,3*]

[1]Department of Earth and Environment, Boston University, Boston, MA
[2]Department of Marine Science, University of North Carolina, Chapel Hill, NC
[3]Department of Biology, Boston University, Boston, MA
[4]U.S. Environmental Protection Agency, Narragansett, RI
[5] Division of Plant Science, University of Dundee at the James Hutton Institute, Dundee, UK
[6]Climate Change Cluster, University of Technology Sydney, Ultimo, New South Wales, Australia
[7]School of Biological Sciences, University of Western Australia, Crawley, New South Wales, Australia
[8]Division of Math and Science, Babson College, Wellesley, MA, USA

Corresponding Author: Robinson W. Fulweiler, Ph: 617-358-5466, rwf@bu.edu

Total Word Count: 2718
Word Count by Section:
Introduction: 615
Materials and Methods: 681
Results: 160
Discussion: 1262
# of Figures: 2 – both color
# of Tables: 2
No supporting Information

Summary

- The silica rich walls of diatoms provide a variety of benefits including structural support, defense from herbivory, enhanced nutrient uptake, and protection from UV radiation. While much research has focused on describing silica concentrations in diatoms, silica concentrations in marine macrophytes remain largely unknown.
- We investigated biogenic silica (BSi) concentrations in 12 macroalgae genera from two temperate estuaries. From a subset of macroalgae samples we also measured percent carbon (%C), and from one of the estuaries we measured delta carbon thirteen ($\delta^{13}C$).
- Our results demonstrate that macroalgae contain significant amounts of BSi ranging between 0.13 to 39 %BSi by mass – concentrations on par with freshwater macrophytes and terrestrial plants. BSi concentrations varied across phyla, and this difference was driven by high concentrations in Rhodophyta. Significant negative relationships were observed between %C and %BSi as well as $\delta^{13}C$ and %BSi.
- Based on these temperate macroalgae values we estimate a potential average global macroalgae uptake rate up to 0.71 Tmol silicon (Si) per year, an amount equivalent to ~10% of the Si entering the oceans from rivers annually. We conclude that macroalgae are an overlooked but potentially important sink of Si in marine ecosystems.

Introduction

Across the marine landscape – from estuaries to the open ocean, biota take up silicon (Si) as monosilicic acid ($Si(OH_4)$) and deposit it into their tissues as biogenic silica (BSi, SiO_2). Along the coast, vegetated ecosystems such as salt marshes and mangroves sequester a significant amount of Si in their tissues and likely help regulate the availability of Si in surrounding waters (Carey & Fulweiler, 2014; Elizondo *et al.*, 2021). Si is also accumulated by sponges, euglyphid amoebae, radiolarians, silicoflagellates, choanoflagellates, as well as a few coccolithophores, Prasinophyceae, and picocyanobacteria (Raven & Giordano, 2009; Gadd & Raven, 2010; Baines *et al.*, 2012). The dominant driver of coastal (and open ocean) Si cycling however, is generally thought to be diatoms. These siliceous phytoplankton require Si on a 1:1 molar ratio with nitrogen (N). Diatoms are responsible for 40-50% of global marine primary production (Field *et al.*, 1998; Rousseaux & Gregg, 2013) and form the base of the marine food web in many parts of the ocean, especially coastal temperate regions (Irigoien *et al.*, 2002).

Macroalgae are also important primary producers, particularly in shallow coastal marine ecosystems, with global net primary production of 80-210 Tmol C per year (Raven, 2018). Macroalgae act as a food source for grazers (Horne *et al.*, 1994), and play a large role in altering the cycling of nutrients such as N and phosphorus (P) (Hersh, 1995). Many estuaries have experienced a shift towards macroalgae as the dominant group of primary producers over the past several decades (Valiela *et al.*, 1992; Hauxwell *et al.*, 2001; Potter *et al.*, 2021). This is due to the ability of macroalgae to thrive in nutrient rich systems, displacing other primary producers by way of rapid uptake of N and P and shading of photosynthetic organisms below (e.g., the seagrass *Zostera* (Valiela *et al.*, 1992, 1997; Peckol *et al.*, 1994).

The role of macroalgae on Si availability however, is largely unconstrained with only a few published studies reporting BSi concentrations. Work on freshwater macrophytes found BSi concentrations ranged from 0.2 to 2.8 (%BSi by dry wt.) and %BSi was positively correlated to water flow (Schoelynck *et al.*, 2010, 2012). Research from four decades ago on freshwater macroalgae demonstrated more rapid growth in *Cladophora glomerata* when Si was added to the growth medium (Moore & Traquair, 1976). The stipe of *Ecklonia cava* was reported to contain BSi concentrations of 13.35 µg per gram dry mass (0.0013 %BSi) and the tissue of *Delisea fimbriaia* contained 1530 µg per gram dry mass (0.15 %BSi) (Fu *et al.*, 2000). More recently, BSi concentrations of the sporophytes of kelp, *Saccharian japonica*, was found to vary by

location on the blade (Mizuta & Yasui, 2012) and to increase when *S. japonica* experienced various stresses (Mizuta *et al.*, 2021). Similarly, BSi concentrations of *Pyropia yezoensis* increased when expose to increase temperature and reached a concentration of 30% BSi (Le *et al.*, 2019).

We hypothesized that marine macroalgae may contain significant amounts of Si in their biomass and thus could impact the Si cycle of coastal ecosystems. To determine the extent to which marine macroalgae are a reservoir of Si, we quantified BSi concentrations from 12 macroalgae genera from two temperate estuaries (Narragansett Bay, RI and Waquoit Bay, MA, USA) and from a subset of samples we measured macroalgae percent carbon (%C). Finally, from one of the estuaries we used macroalgae $\delta^{13}C$ values, which can be used as a proxy for identifying CO_2 or HCO_3^- source in photosynthesis, to infer presence/absence of carbon concentration mechanisms (Raven *et al.*, 2002), and as an indicator of productivity (Oczkowski *et al.*, 2010). We then examined the relationship between BSi concentrations and macroalgae $\delta^{13}C$ to better understand mechanisms driving BSi uptake.

Materials and Methods

Macroalgae Sampling

We collected macroalgae samples from Waquoit Bay (Massachusetts, USA) from the surface water using a sampling net, or from the bottom water using a Ponar benthic grab (523 cm^2). Three sites were sampled (Child's River Estuary, Metoxit Point, and Sage Lot Pond) on four separate occasions (September 2015, October 2015, and twice in June 2016). We also collected macroalgae samples by hand from 19 sites in Narragansett Bay (Rhode Island, USA) on one occasion (September 2015). Narragansett Bay samples were collected from just below the water surface at the bases of lighthouses and rocky outcrops during low tide. All samples were stored in plastic containers and bags in the dark until return to the lab where they were then frozen until analysis.

BSi, C:N, and $\delta^{13}C$ analysis

Prior to BSi analysis the macroalgae samples were separated by genus and, where possible, to species. Next, they were rinsed with deionized water and gently brushed to remove any visible epiphytes. Samples were then placed in ethanol-cleaned aluminum tins, and dried at

60 °C for a minimum of 72 h. Following drying, the sample was ground and homogenized using a Wig-L-Bug™.

We quantified BSi concentrations in the ground macroalgae samples using the wet alkaline extraction technique in 1% sodium carbonate (Na_2CO_3) solution wet alkaline digestion method (DeMaster, 1981; Conley & Schelske, 2002). Briefly, 30 mg of ground sample (weighed to a precision of 0.1 mg) was processed in flat bottomed polyethylene bottles. We used a SEAL AA3 Flow Injection Auto Analyzer to determine DSi concentrations of the digestate using the molybdenum blue colorimetric method (Strickland & Parsons, 1968). We used sodium hexafluorosilicate (Na_2SiF_6) as the silicon standard (Strickland & Parsons, 1968) as well as Hach external standards, to ensure accuracy. All standards were within 4% of expected value, and minimum detection limits during analysis were 0.030 μmol L^{-1}. We then converted DSi concentrations of the digestate back to macroalgae %BSi by mass (Conley & Schelske, 2002). Finally, when reporting carbon to silicon molar ratios (C:Si), we converted our BSi values to Si by multiplying by 0.47, the mass fraction of Si in molecule of SiO_2 (Elizondo *et al.*, 2021).

A subset of the Waquoit Bay macroalgae samples were analyzed for percent C and N using standard methods (Dalsgaard, 2000) and a Eurovector CHN elemental analyzer at the Boston University Stable Isotopes Lab, Boston, Massachusetts, USA. All of the Narragansett Bay samples were analyzed for percent C and N and $\delta^{13}C$ on a Carlo-Erba NA 1500 Series II elemental analyzer interfaced with a Micromass Optima mass spectrometer (Oczkowski *et al.*, 2018).

Data Analysis

All statistical analyses were conducted in R Statistical Software version 3.6.0 (R-Development-Team, 2014). We considered the results of statistical tests to be significant when $p \leq 0.05$. Figures were made using the *ggplot2* (Wickham, 2016) and *cowplot* (Wilke, 2019). We determined data distributions using the *fitdistrplus* package (Marie *et al.*, 2015) by comparing whether the data was best described by a normal, lognormal, or gamma distribution. %BSi data were best described by a lognormal distribution, and C:Si best fit a gamma distribution. All measured $\delta^{13}C$ values were negative, so we mirrored them around zero to test their distribution, which we found to be normal.

To compare the relationship of macroalgae %BSi across phyla and genera, we used a generalized linear mixed model (GLMM) approach via the *lme4* package (Bates *et al.*, 2015). In each GLMM, we set phylum, or genus as a fixed effect, and the estuary as a random effect. %BSi data were lognormally distributed, so we first applied a log transformation to the %BSi data prior to constructing the model, but the resulting models had heteroscedastic residuals. We re-made the model using a gamma family with a log-link, after which the residual distribution improved (Zuur *et al.*, 2009). Following model construction, we compared groups using pairwise least-square means tests using the *emmeans* package (Lenth, 2018). We tested for relationships between %C and BSi concentrations and between log transformed BSi concentrations and $\delta^{13}C$ using linear regressions. We tested for correlations between %BSi or %C with latitude using Spearman correlation.

Results

Individual macroalgae samples varied widely in BSi concentration from a low of 0.13% in *Laminaria* to a high of 39.4% in *Polysiphonia* (Figure 1). At the phylum level, Rhodophyta had significantly ($p < 0.0001$) higher BSi concentrations compared to Ochrophyta and Chlorophyta, and Chlorophyta had significantly ($p < 0.0001$) higher BSi concentrations compared to Ochrophyta. The high Rhodophyta BSi concentrations were primarily driven by the genera *Cystoclonium* and *Polysiphonia,* which exhibited BSi concentrations almost ten times that of the other macroalgae samples, regardless of phylum (Table 1). Genera BSi concentrations within Chlorophyta and Ochrophyta were not significantly different from each other. Genera within Rhodophyta were statistically different from each other (Table 2).

BSi concentrations were significantly negatively related to %C ($p < 0.0001$, $R^2 = 0.48$; Figure 2a). There was also a significant negative relationship between log transformed macroalgae BSi concentrations and $\delta^{13}C$ ($p < 0.01$, $R^2 = 0.42$; Figure 2b) where $\delta^{13}C$ was more depleted as BSi concentrations increased.

Discussion

BSi concentrations vary widely in Si requiring marine biota. For example, even within a single diatom species BSi concentrations can vary by an order of magnitude (Taylor, 1985; Claquin *et al.*, 2002). Similarly, BSi concentrations in these macroalgae also varied widely

across genera (Figure 1). In general, the BSi concentrations (4.2% (mean) ± 0.84 (SE)) in macroalgae exceeded or were on par to values reported for salt marsh grasses collected in Narragansett Bay and other nearby estuaries (*Spartina patens*: 0.63 ± 0.38 %BSi by wt. and *Spartina alterniflora*: 0.57±0.24 %BSi by wt. (Carey & Fulweiler, 2014)). These macroalgae BSi concentrations are also generally higher than those reported for leaves of seagrasses (e.g., 0.06 – 0.7% (Vonk *et al.*, 2018)). Overall, there was low variability within phylum, except for Rhodophyta where BSi concentrations varied widely. The high variability of BSi concentrations may be driven by different responses of macroalgae to environmental conditions and/or stressors.

The siliceous wall in diatoms confers a range of benefits including providing structural support for their large protoplast (Raven & Waite, 2004; Finkel & Kotrc, 2010), increasing nutrient uptake (Mitchell *et al.*, 2013), aiding light harvest (Romann *et al.*, 2015), protection from UV radiation (Aguirre *et al.*, 2018), reducing herbivory (Pančić *et al.*, 2019), and possibly limiting viral infection (Raven and Waite, 2004). The large variations in diatom Si concentrations is thought to be driven in part by environmental conditions such as light and nutrient availability (Brzezinski, 1985) as well as grazing pressure (Pančić et al. 2019). A recent study reported that the cell wall of diatoms thickened under copepod grazing pressure, and that silica deposition decreased with increasing diatom growth rates (Pančić et al. 2019). Pančić et al. propsed, that their results suggest diatoms use Si as a defense but that this defense comes at a cost. Macroalgae may also be taking up Si for similar reasons and potentially they too may need to sacrifice growth for defense or vice versa – defense for growth.

We can examine some of these factors a bit more closely for the macroalgae samples from Narragansett Bay, which were collected from sites along a gradient of potential stressors. Narragansett Bay is orientated in a roughly north-south position with lower salinity, higher inorganic nutrient concentrations, including dissolved silica, and higher rates of primary production in the northern reaches of the bay, where light is also typically more limited (Oviatt *et al.*, 2002; Smayda & Borkman, 2008; Nixon *et al.*, 2009). While macroalgae BSi concentrations did not vary by location within Narragansett Bay as a whole, BSi concentrations for Rhodophyta alone significantly decreased ($r=-0.47$, $p = 0.034$), while %C increased ($r= 0.62$, $p = 0.008$) along this north-south gradient. That is, the Rhodophyta samples collected in northern Narragansett Bay incorporated more Si into their biomass, and less C. Overall, we found that BSi concentrations increase as macroalgae %C decreases – suggesting that macroalgae may

substitute Si in for C (Figure 2a). This relationship was again driven by macroalgae in the phylum Rhodophyta, whereas samples for Chlorophyta and Ochrophyta tended to vary less in terms of BSi concentration and %C. An inverse relationship between C and BSi concentration has been reported for a variety of flowering plant species (e.g., *Phragmites australis*: (Schaller *et al.*, 2012), *Triticum aestivum*: (Neu *et al.*, 2017)) as well as for grassland ecosystems (Quigley *et al.*, 2020). Additionally, Schoelynck et al. (2010) found a negative relationship between cellulose and BSi concentrations for freshwater macrophytes (Schoelynck et al. 2010). Incorporating Si is an energetically cheaper mechanism for structural support (Raven, 1983) while also providing additional benefits. These findings suggest that certain macroalgae, primarily in the phylum Rhodophyta, may take up Si in response to *in situ* availability and/or environmental stressors, similar to what is observed for diatoms. The inverse relationship between BSi concentration and %C may also prove to be useful for scaling. That is, %C data is more widely available for macroalgae than BSi concentration. If this irelationship holds for more species and more locations then we may be able to use the more abundant %C data to predict how much Si is taken up across space and time.

We also observed a negative relationship between $\delta^{13}C$ and BSi concentrations (Figure 2b). These relationships described a substantial portion of the variance in $\delta^{13}C$, which can be used to help understand macroalgae photosynthetic pathways (Giordano *et al.*, 2005; Marconi *et al.*, 2011; Lovelock *et al.*, 2020) and environmental conditions influencing macroalgae growth (Dudley *et al.*, 2010). The $\delta^{13}C$ values reported here (-12.60‰ to -23.54‰) are well within the range reported for macroalgae (Maberly *et al.*, 1992; Raven *et al.*, 2005; Lovelock *et al.*, 2020). These values also suggest that inorganic C entry is driven by a combination of carbon dioxide diffusion directly to Rubisco as well as through the carbon concentrating mechanisms (CCMs). There is a clear pattern with phylum $\delta^{13}C$ and BSi concentrations (Figure 2b). At this point we are uncertain what mechanism is driving the pattern between $\delta^{13}C$ and BSi concentration. Perhaps, it is simply a correlation with – as the well-worn phrase goes – no causation. Alternatively, it may provide insight in how and why macroalgae take up Si. The more negative $\delta^{13}C$ associated with higher BSi is consistent with a large fraction of the inorganic C being pumped into cells in organism with carbon concentrating mechanisms, or diffusive carbon dioxide entry, allowing discrimination against $\delta^{13}C$ by Rubisco. All other things being equal, that may indicate lower growth rates and hint at the tradeoffs of incorporating Si. However, we

cannot at this time connect the $\delta^{13}C$ directly to BSi concentrations as the factors driving $\delta^{13}C$ signatures are upstream of allocation of photosynthate to growth or Si uptake.

Finally, uptake of Si by macroalgae may help promote Si limitation in estuaries, especially if they are actively sequestering it, and therefore competing with diatoms for Si. We can estimate the amount of Si taken up by macroalgae by using the C:Si ratio measured here, and literature reported values for global macroalgae primary productivity. Annually, global macroalgae net primary production (and C uptake) ranges from 80-210 Tmol C per year (Raven, 2018). Scaling this by the mean macroalgae C to Si molar ratio measured in this study (295.6), we calculate an average global macroalgae uptake rate between 0.27-0.71 Tmol Si per year. The maximum value accounts for almost 10% of the Si entering the ocean from rivers and over 40% of the annual uptake of Si by sponges (Tréguer *et al.*, 2021). This is likely a conservative estimate, as using the median C:Si molar ratio in this study (157.4) would increase global macroalgae uptake to between 0.5-1.33 Tmol Si per year. In this case, the maximum value would account for 16% of the Si entering the ocean from rivers and almost 80% of the annual uptake of Si by sponges. Potentially these values could be higher. For example, a recent eDNA studied reported that Rhodophyta, the genera with the highest BSi concentrations in this study, were the dominant genera of macroalgae found in the worlds oceans (Ortega *et al.*, 2019). Of course, our calculations are rough approximation based on temperate macroalgae only. We anticipate the BSi concentrations may vary by geographic location, seasonality, and exposure to stress. Regardless, this study suggests marine macroalgae are a potentially important, yet largely ignored, sink of Si in marine ecosystems. This sink may be particularly in important in systems that are heavily fertilized with inorganic N and P, where macroalgae come to dominate. Perhaps macroalgae Si uptake contributes to Si limitation in coastal systems, thereby exacerbating the negative impacts of eutrophication.

Acknowledgements

This work was funded in part by a Woods Hole Sea Grant to a grant to RWF. This work was also funded through Boston University's Undergraduate Research Opportunities Program through grant support to MY. We thank the Waquoit Bay National Estuarine Research Reserve staff, particularly Jim Rassman, for their assistance in sampling in Waquoit Bay. Additionally, we thank Alia Al-Haj, Sarah Fabbricotti, and Mac Marston for their assistance in sample analysis

and processing. Finally we thank Serdar Korur whose code we adapted for Figure 1. The University of Dundee is a registered Scottish charity, No. SC015096. The views expressed in this article are those of the authors and do not necessarily reflect the views or policies of the U.S. Environmental Protection Agency (EPA). Any mention of trade name and products does not imply an endorsement by the U.S. Government or the U.S. EPA. The EPA does not endorse any commercial products, services, or enterprises.

Author Contributions

MRY, SQF, and RWF conceived of this study. MYR and SQF conducted field and laboratory analysis for all Waquoit Bay samples and for the BSi analysis for the Narragansett Bay samples. AO collected the Narragansett Bay samples and conducted the %C and isotope analysis. NER and RWF conducted the statistical analysis. MRY, SQF, and RWF wrote the original draft. All authors contributed to manuscript idea development, writing, and editing.

Data Availabilty

All data is available via: https://doi.org/10.6084/m9.figshare.15113139.v1

References:

Aguirre LE, Ouyang L, Elfwing A, Hedblom M, Wulff A, Inganäs O. **2018**. Diatom frustules protect DNA from ultraviolet light. *Scientific Reports* **8**: 1–6.

Baines SB, Twining BS, Brzezinski MA, Krause JW, Vogt S, Assael D, McDaniel H. **2012**. Significant silicon accumulation by marine picocyanobacteria. *Nature Geoscience* **5**: 886–891.

Bates D, Maechler M, Bolker B, Walker S. **2015**. Fitting linear mixed-effects models using *lme4*. *Journal of Statistical Software* **67**: 1–48.

Brzezinski MA. **1985**. The Si: C: N ratio of marine diatoms: interspecific variability and the effect of some environmental variables 1. *Journal of Phycology* **21**: 347–357.

Carey JC, Fulweiler RW. **2014**. Salt marsh tidal exchange increases residence time of silica in estuaries. *Limnology and Oceanography* **59**: 1203–1212.

Claquin P, Martin-Jézéquel V, Kromkamp JC, Veldhuis MJW, Kraay GW. **2002**. Uncoupling of silicon compared with carbon and nitrogen metabolisms and the role of the cell cycle in continuous cultures of Thalassiosira pseudonana (Bacillariophyceae) under light, nitrogen, and phosphorus control1. *Journal of Phycology* **38**: 922–930.

Conley DJ, Schelske CL. **2002**. Biogenic Silica. In: Tracking Environmental Change Using Lake Sediments. Dordrecht: Kluwer Academic Publishers, 281–293.

Dalsgaard T. **2000**. *Protocol handbook for NICE-nitrogen cycling in estuaries*.

DeMaster DJ. **1981**. The supply and accumulation of silica in the marine environment. *Geochimica et Cosmochimica Acta* **45**: 1715–1732.

Dudley BD, Barr NG, Shima JS. **2010**. Influence of light intensity and nutrient source on δ13C and δ15N signatures in Ulva pertusa. *Aquatic Biology* **9**: 85–93.

Elizondo EB, Carey JC, Al-Haj AN, Lugo AE, Fulweiler RW. **2021**. High Productivity Makes Mangroves Potentially Important Players in the Tropical Silicon Cycle. *Frontiers in Marine Science* **8**: 450.

Field CB, Behrenfeld MJ, Randerson JT, Falkowski P. **1998**. Primary production of the biosphere: integrating terrestrial and oceanic components. *science* **281**: 237–240.

Finkel Z V, Kotrc B. **2010**. Silica use through time: macroevolutionary change in the morphology of the diatom fustule. *Geomicrobiology Journal* **27**: 596–608.

Fu FF, Akagi T, Yabuki S, Iwaki M, Ogura N. **2000**. Distribution of rare earth elements in seaweed: implication of two different sources of rare earth elements and silicon in seaweed. *Journal of Phycology* **36**: 62–70.

Gadd GM, Raven JA. **2010**. Geomicrobiology of eukaryotic microorganisms. *Geomicrobiology Journal*.

Giordano M, Beardall J, Raven JA. **2005**. CO 2 concentrating mechanisms in algae: mechanisms, environmental modulation, and evolution. *Annu. Rev. Plant Biol.* **56**: 99–131.

Hauxwell J, Cebrián J, Furlong C, Valiela I. **2001**. Macroalgal canopies contribute to eelgrass (Zostera marina) decline in temperate estuarine ecosystems. *Ecology* **82**: 1007–1022.

Hersh DA. **1995**. Effects of nutrient loading on species composition of vegetation in a New England coastal lagoon system and salt marsh.

Horne A, McClelland J, Valiela I. **1994**. The growth and consumption of macroalgae in estuaries: the role of invertebrate grazers along a nutrient gradient in Waquoit Bay,

Massachusetts. *The Biological Bulletin* **187**: 279–280.

Irigoien X, Harris RP, Verheye HM, Joly P, Runge J, Starr M, Pond D, Campbell R, Shreeve R, Ward P. **2002**. Copepod hatching success in marine ecosystems with high diatom concentrations. *Nature* **419**: 387–389.

Le B, Nadeem M, Yang S-H, Shin J-A, Kang M-G, Chung G, Sun S. **2019**. Effect of silicon in Pyropia yezoensis under temperature and irradiance stresses through antioxidant gene expression. *Journal of Applied Phycology* **31**: 1297–1302.

Lenth R. **2018**. *emmeans*: Estimated marginal means, aka least-squares means. R package version 1.2.3.

Lovelock CE, Reef R, Raven JA, Pandolfi JM. **2020**. Regional variation in δ 13C of coral reef macroalgae. *Limnology and Oceanography* **65**: 2291–2302.

Maberly SC, Raven JA, Johnston AM. **1992**. Discrimination between 12 C and 13 C by marine plants. *Oecologia* **91**: 481–492.

Marconi M, Giordano M, Raven JA. **2011**. Impact of taxonomy, geography, and depth on δ13C and δ15N variation in a large collection of macroalgae. *Journal of phycology* **47**: 1023–1035.

Marie A, Delignette-muller L, Dutang C, Denis J, Delignette-muller MML. **2015**. *fitdistrplus*: An R package for fitting fistributions. *Journal of Statistical Software* **64**: 1–34.

Mitchell JG, Seuront L, Doubell MJ, Losic D, Voelcker NH, Seymour J, Lal R. **2013**. The role of diatom nanostructures in biasing diffusion to improve uptake in a patchy nutrient environment. *PLoS One* **8**: e59548.

Mizuta H, Uji T, Yasui H. **2021**. Extracellular silicate uptake and deposition induced by oxidative burst in Saccharina japonica sporophytes (Phaeophyceae). *Algal Research* **58**: 102369.

Mizuta H, Yasui H. **2012**. Protective function of silicon deposition in Saccharina japonica sporophytes (Phaeophyceae). *Journal of Applied Phycology* **24**: 1177–1182.

Moore LF, Traquair JA. **1976**. Silicon, a required nutrient for Cladophora glomerata (L) K??tz. (Chlorophyta). *Planta* **128**: 179–182.

Neu S, Schaller J, Dudel EG. **2017**. Silicon availability modifies nutrient use efficiency and content, C: N: P stoichiometry, and productivity of winter wheat (Triticum aestivum L.). *Scientific Reports* **7**: 1–8.

Nixon SW, Fulweiler RW, Buckley B a., Granger SL, Nowicki BL, Henry KM. **2009**. The

impact of changing climate on phenology, productivity, and benthic–pelagic coupling in Narragansett Bay. *Estuarine, Coastal and Shelf Science* **82**: 1–18.

Oczkowski AJ, Pilson MEQ, Nixon SW. **2010**. A marked gradient in ??13C values of clams Mercenaria mercenaria across a marine embayment may reflect variations in ecosystem metabolism. *Marine Ecology Progress Series* **414**: 145–153.

Oczkowski A, Schmidt C, Santos E, Miller K, Hanson A, Cobb D, Krumholz J, Pimenta A, Heffner L, Robinson S. **2018**. How the distribution of anthropogenic nitrogen has changed in Narragansett Bay (RI, USA) following major reductions in nutrient loads. *Estuaries and Coasts* **41**: 2260–2276.

Ortega A, Geraldi NR, Alam I, Kamau AA, Acinas SG, Logares R, Gasol JM, Massana R, Krause-Jensen D, Duarte CM. **2019**. Important contribution of macroalgae to oceanic carbon sequestration. *Nature Geoscience* **12**: 748–754.

Oviatt C, Keller A, Reed L. **2002**. Annual primary production in Narragansett Bay with no bay-wide winter–spring phytoplankton bloom. *Estuarine, Coastal and Shelf Science* **54**: 1013–1026.

Pančić M, Torres RR, Almeda R, Kiørboe T. **2019**. Silicified cell walls as a defensive trait in diatoms. *Proceedings of the Royal Society B* **286**: 20190184.

Peckol P, DeMeo-Anderson B, Rivers J, Valiela I, Maldonado M, Yates J. **1994**. Growth, nutrient uptake capacities and tissue constituents of the macroalgae Cladophora vagabunda and Gracilaria tikvahiae related to site-specific nitrogen loading rates. *Marine biology* **121**: 175–185.

Potter IC, Rose TH, Huisman JM, Hall NG, Denham A, Tweedley JR. **2021**. Large variations in eutrophication among estuaries reflect massive differences in composition and biomass of macroalgal drift. *Marine Pollution Bulletin* **167**: 112330.

Quigley KM, Griffith DM, Donati GL, Anderson TM. **2020**. Soil nutrients and precipitation are major drivers of global patterns of grass leaf silicification. *Ecology* **101**: e03006.

R-Development-Team. **2014**. R: A language and environment for statistical computing. *R Foundation for Statistical Computing*.

Raven JA. **1983**. The transport and function of silicon in plants. *Biological reviews* **58**: 179–207.

Raven J. **2018**. Blue carbon: Past, present and future, with emphasis on macroalgae. *Biology Letters*.

Raven JA, Ball LA, Beardall J, Giordano M, Maberly SC. **2005**. Algae lacking carbon-concentrating mechanisms. *Canadian Journal of Botany* **83**: 879–890.

Raven JA, Giordano M. **2009**. Biomineralization by photosynthetic organisms: Evidence of coevolution of the organisms and their environment? *Geobiology* **7**: 140–154.

Raven JA, Johnston AM, Kübler JE, Korb R, McInroy SG, Handley LL, Scrimgeour CM, Walker DI, Beardall J, Vanderklift M. **2002**. Mechanistic interpretation of carbon isotope discrimination by marine macroalgae and seagrasses. *Functional Plant Biology* **29**: 355–378.

Raven JA, Waite AM. **2004**. The evolution of silicification in diatoms: inescapable sinking and sinking as escape? *New phytologist* **162**: 45–61.

Romann J, Valmalette J-C, Chauton MS, Tranell G, Einarsrud M-A, Vadstein O. **2015**. Wavelength and orientation dependent capture of light by diatom frustule nanostructures. *Scientific reports* **5**: 1–6.

Rousseaux CS, Gregg WW. **2013**. Interannual variation in phytoplankton primary production at a global scale. *Remote Sensing*.

Schaller J, Brackhage C, Gessner MO, Bäuker E, Gert Dudel E. **2012**. Silicon supply modifies C: N: P stoichiometry and growth of Phragmites australis. *Plant Biology* **14**: 392–396.

Schoelynck J, Bal K, Backx H, Okruszko T, Meire P, Struyf E. **2010**. Silica uptake in aquatic and wetland macrophytes: A strategic choice between silica, lignin and cellulose? *New Phytologist* **186**: 385–391.

Schoelynck J, De Groote T, Bal K, Vandenbruwaene W, Meire P, Temmerman S. **2012**. Self-organised patchiness and scale-dependent bio-geomorphic feedbacks in aquatic river vegetation. *Ecography* **35**: 760–768.

Smayda TJ, Borkman DG. **2008**. Nutrient and plankton dynamics in Narragansett Bay. In: Science for ecosystem-based management. Springer, 431–484.

Strickland J, Parsons T. **1968**. *A practical handbook of seawater analysis*. Fisheries Research Board of Canada.

Taylor NJ. **1985**. Silica incorporation in the diatom Cosinodiscus granii as affected by light intensity. *British Phycological Journal* **20**: 365–374.

Tréguer PJ, Sutton JN, Brzezinski M, Charette MA, Devries T, Dutkiewicz S, Ehlert C, Hawkings J, Leynaert A, Liu SM. **2021**. Reviews and syntheses: The biogeochemical cycle of silicon in the modern ocean. *Biogeosciences* **18**: 1269–1289.

Valiela I, Foreman K, LaMontagne M, Hersh D, Costa J, Peckol P, DeMeo-Andreson B, D'Avanzo C, Babione M, Sham C-H. **1992**. Couplings of watersheds and coastal waters:

sources and consequences of nutrient enrichment in Waquoit Bay, Massachusetts. *Estuaries* **15**: 443–457.

Valiela I, McClelland J, Hauxwell J, Behr PJ, Hersh D, Foreman K. **1997**. Macroalgal blooms in shallow estuaries: controls and ecophysiological and ecosystem consequences. *Limnology and oceanography* **42**: 1105–1118.

Vonk JA, Smulders FOH, Christianen MJA, Govers LL. **2018**. Seagrass leaf element content: A global overview. *Marine Pollution Bulletin*.

Wickham H. **2016**. ggplot2*: Elegant Graphics for Data Analysis*. New York: Springer-Verlag.

Wilke C. **2019**. *cowplot*: Streamlined plot theme and plot annotations for '*ggplot2*'. R package version 1.0.0.

Zuur A, Ieno EN, Walker N, Saveliev AA, Smith GM. **2009**. *Mixed effects models and extensions in ecology with R*. Springer Science & Business Media.

442 **Table 1:** Mean (± standard error) biogenic silica concentrations (%BSi as SiO_2 dry wt.) in
443 macroalgae from Narragansett Bay (RI, USA) and Waquoit Bay (MA, USA).
444

Phylum	Genera	n	%BSi
Chlorophyta	*Cladophora*	7	1.50 ± 0.23
	Codium	1	1.57
	Enteromorpha	3	1.60 ± 1.06
	Ulva	31	1.63 ± 0.28
Ochrophyta	*Ascophyllum*	1	0.61
	Fucus	7	0.34 ± 0.08
	Laminaria	1	0.13
	Saccharina	1	0.24
Rhodophyta	*Chondrus*	5	1.16 ± 0.43
	Cystoclonium	1	22.96
	Gracilaria	10	2.37 ± 0.68
	Grateloupia	5	2.62 ± 1.06
	Polysiphonia	10	21.15 ± 3.07

445
446

447 **Table 2:** P-values from least square mean comparisons of biogenic silica (%BSi as SiO_2 per dry wt.) content of macroalgae genera.
448 Significant differences ($p \leq 0.05$) are bolded. See Table 1 for mean BSi concentrations.

	Chondrus	*Cladophora*	*Codium*	*Cystoclonium*	*Enteromorpha*	*Fucus*	*Gracilaria*	*Grateloupia*	*Laminaria*	*Polysiphonia*	*Saccharina*	*Ulva*
Ascophyllum	0.999	0.996	1.00	**0.031**	0.996	1.00	0.876	0.853	0.957	**< 0.001**	1.00	0.985
Chondrus		1.00	1.00	**0.015**	1.00	0.179	0.874	0.883	0.237	**< 0.001**	0.757	0.999
Cladophora			1.00	**0.033**	1.00	**0.011**	0.990	0.988	0.089	**< 0.001**	0.492	1.00
Codium				0.336	1.00	0.773	1.00	1.00	0.444	**0.045**	0.847	1.00
Cystoclonium					0.090	**< 0.001**	0.151	0.268	**< 0.001**	1.00	**0.001**	**0.027**
Enteromorpha						0.111	1.00	1.00	0.137	**< 0.001**	1.00	1.00
Fucus							**< 0.001**	**< 0.001**	0.991	**< 0.001**	1.00	**< 0.001**
Gracilaria								1.00	*0.011*	**< 0.001**	0.135	0.978
Grateloupia									*0.012*	**< 0.001**	0.136	0.984
Laminaria										**< 0.001**	1.00	**0.039**
Polysiphonia											**< 0.001**	**< 0.001**
Saccharina												0.330

449

Figure 1: Median (black star) and the interquartile range of biogenic silica (%BSi as SiO_2 per dry wt.) concentrations of macroalgae by genus. Individual sample values are also shown as circles (Chlorophyta: green, Ochrophyta: brown, Rhodoyphta: red).

Figure 2: Relationship between a) biogenic silica (%BSi as SiO_2 per dry wt.) and carbon (%C) content b) biogenic silica and $\delta^{13}C$ in macroalgae samples collected from Narragansett Bay, RI (USA). Samples are color coded by phylum (Chlorophyta: green, Ochrophyta: brown, Rhodophyta: red). The shaded area around the regression line is the 95% confidence interval.

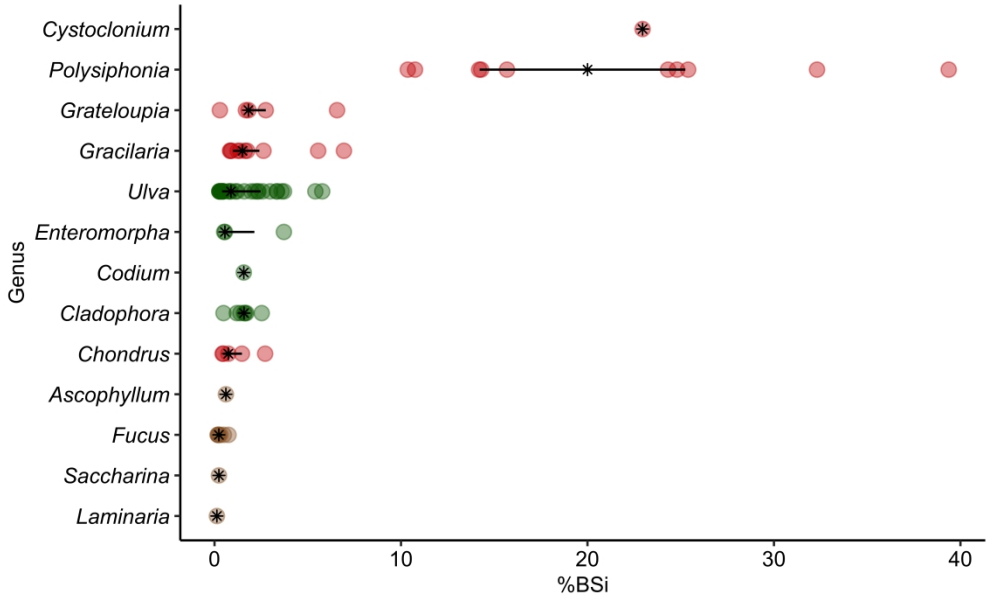

Figure 1: Median (black star) and the interquartile range of biogenic silica (%BSi as SiO2 per dry wt.) concentrations of macroalgae by genus. Individual sample values are also shown as circles (Chlorophyta: green, Ochrophyta: brown, Rhodoyphta: red).

2063x1270mm (72 x 72 DPI)

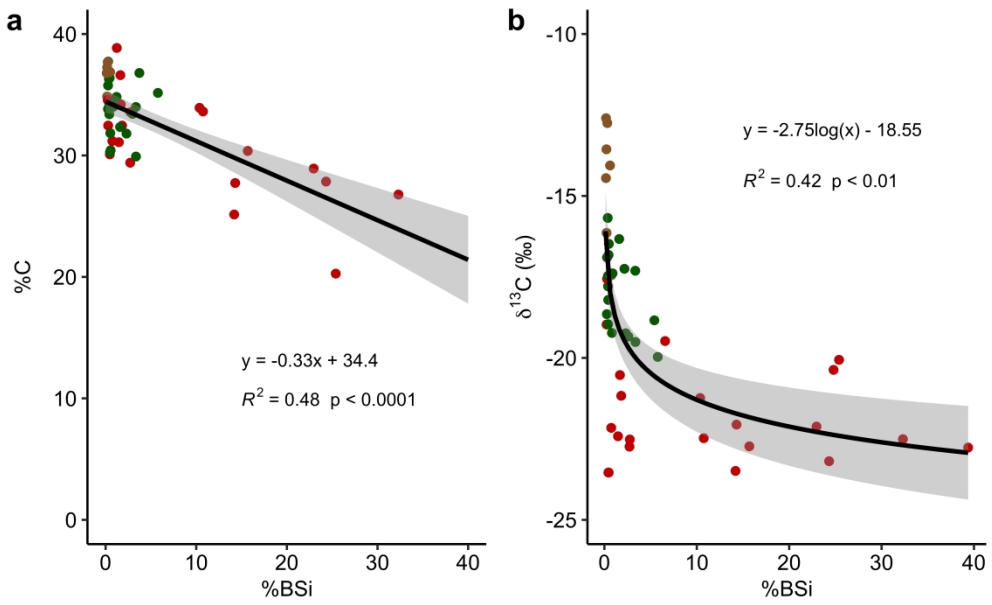

Figure 2: Relationship between a) biogenic silica (%BSi as SiO2 per dry wt.) and carbon (%C) content b) biogenic silica and δ13C in macroalgae samples collected from Narragansett Bay, RI (USA). Samples are color coded by phylum (Chlorophyta: green, Ochrophyta: brown, Rhodophyta: red). The shaded area around the regression line is the 95% confidence interval.

2063x1270mm (72 x 72 DPI)